# Some Examples of the Use of IR Spectroscopy in Mineralogical Studies

# 1

## 1.1 Characteristic Bands in IR Spectra of Vesuvianite-Group Minerals

Vesuvianite-group minerals (VGM) are widespread and occur in different geological formations including regional metamorphic rocks, skarns, rodingites, etc. Specific crystal-chemical features of these minerals reflect conditions of their crystallization. As a rule, high-temperature VGM have high-symmetry structures (space group *P4/nnc*), whereas low-temperature samples are characterized by the symmetry *P4/n* or *P4nc* (Allen and Burnham 1992). The simplified crystal-chemical formula of VGM is $X_{18}(X'Y1)Y2_4Y3_8T_{0-5}(SiO_4)_{10}(Si_2O_7)_4O_{1-2}W_9$ where *X*, *X′* = Ca, Na, K, $Fe^{2+}$, and *REE* (cations with coordination numbers from 7 to 9); *Y*1–*Y*3 = Al, Mg, $Fe^{2+}$, $Fe^{3+}$, $Mn^{2+}$, $Mn^{3+}$, Ti, Cr, Cu, Zn; *T* = B, Al, □; *W* = OH, F, O. The *Y*1 cations have tetragonal-pyramidal coordination, whereas the *Y*2 and *Y*3 cations occur in octahedra.

IR spectra of VGM are discussed in numerous publications (Paluszkiewicz and Żabiński 1992; Groat et al. 1995; Kurazhkovskaya and Borovikova 2003; Kurazhkovskaya et al. 2005; Borovikova and Kurazhkovskaya 2006); however, in most cases their interpretation is ambiguous. We have obtained IR spectra of 33 VGM samples from different kinds of localities which have been preliminarily investigated in detail using electron microprobe (including determination of boron), single-crystal X-ray structural analysis, DSC, $^{27}Al$ NMR, ICP-MS, and Mössbauer spectroscopy. As a result, characteristic IR bands corresponding to different local situations in the structures of VGM have been revealed. Data on crystal structures, crystal chemistry, and IR spectra of these samples are published by Britvin et al. (2003), Panikorovskii et al. (2016a–d, 2017a–d), and Aksenov et al. (2016). The most important results of this investigation are listed below in comparison with data published elsewhere.

### 1.1.1 O–H-Stretching Vibrations

The following empirical correlations between O–H stretching frequencies in IR spectra of minerals and O···O and H···O distances (from structural data) were established by E. Libowitzky (1999):

$$\nu\left(\mathrm{cm}^{-1}\right) = 3592 - 304 \cdot 10^{9} \cdot \exp\left[-d(\mathrm{O}\cdots\mathrm{O})/0.1321\right] \quad (1.1)$$

$$\nu\left(\mathrm{cm}^{-1}\right) = 3632 - 1.79 \cdot 10^{6} \cdot \exp\left[-d(\mathrm{H}\cdots\mathrm{O})/0.2146\right] \quad (1.2)$$



N. V. Chukanov, M. F. Vigasina, *Vibrational (Infrared and Raman) Spectra of Minerals and Related Compounds*, Springer Mineralogy, https://doi.org/10.1007/978-3-030-26803-9_1

Two decades ago this publication was of a great importance because it emphasized the existence of such correlations as a general trend. However, over time it became obvious that the Eqs. (1.1) and (1.2) are a very rough approximation and have a restricted applicability. First, it is to be noted that at high frequencies (above 3500 $cm^{-1}$) substantial deviations from the correlations (1.1) and (1.2) are common because O–H stretching frequencies depend not only on O···O and H···O distances, but also on the nature of cations coordinating O–H groups and $H_2O$ molecules, as well as on the angle O–H···O, and the influence of these factors becomes most evident in case of weak hydrogen bonds. The Eqs. (1.1) and (1.2) predict that maximum possible values of O–H stretching frequencies for minerals are 3592 and 3632 $cm^{-1}$ respectively. However, in many minerals including magnesium serpentines, brucite, kaolinite, amphiboles, etc. observed frequencies are much higher and even can exceed 3700 $cm^{-1}$.

In the IR spectra of VGM some absorption bands of O–H stretching vibrations are poorly resolved. In such cases, band component analysis is the most important source of errors and artifacts during data processing because of low correctness of inverse mathematical problems: small errors in experimental data lead to strong uncertainty of the final result. Additional uncertainty is connected with arbitrary choice of the band shape (Gauss, Lorentz, Voigt, or Lorentz-Gauss cross-product function), the number of components, and the acceptable values of the correlation coefficient $R$ (e.g., 0.99, 0.995, or 0.999). This matter is discussed in detail by Chukanov and Chervonnyi (2016) (the section 1.1 "Sources of Errors and Artifacts in IR Spectroscopy of Minerals") where it is shown that different variants of band shape analysis may give a good and almost identical approximation accuracy (say, $R^2 \approx 0.9995$), but lead to totally different results.

For most VGM investigated by Chukanov et al. (2018) there are significant discrepancies between wavenumbers of observed O–H stretching bands and $\nu$ values calculated using correlations suggested by Libowitzky (1999). The above considerations explain why the attempts to apply Eqs. (1.1) and (1.2) to VGM failed.

Groat et al. (1995) distinguished 13 bands of O–H stretching vibrations in IR spectra of VGM, which have absorption maxima at the following wavenumbers ($cm^{-1}$): 3670 (A), 3635 (B), 3596 (C), 3567 (D), 3524 (E), 3487 (F), 3430 (G), 3383 (H), 3240 (I), 3210 (J), 3156 (K), 3120 (L), and 3054 (M). The polarization of these bands with respect to the fourfold $c$ axis is as follows: $E \wedge c < 35°$ for the A–H bands, $E \perp c$ for the I band, and $E \| c$ for the J–M bands (Groat et al. 1995; Bellatreccia et al. 2005). Consequently, the bands A–H and J–M can be assigned to the vibrations of differently coordinated O11–H1 and O10–H2 groups, respectively. The I band was tentatively assigned to O–H stretching vibrations of silanol group (Chukanov et al. 2018).

Our data show that actually significant deviations of the A–M band positions from the "ideal" values indicated by Groat et al. (1995) take place. In particular, IR spectra of many VGM samples contain a band in the range 3440–3470 $cm^{-1}$, i.e., between F and G bands. Taking into account that in the group of 33 chemically and structurally investigated samples the intensity of this band shows distinct positive correlation with Ti content, it was assigned to vibrations of the O11–H1 group coordinated by Ti (Chukanov et al. 2018). Most Ti-rich samples are characterized by the space group *P*4/*nnc*. The only exception is a sample from the Ahkmatovskaya open pit, South Urals with 1.54 *apfu* Ti, space group *P*4/*n* showing bands at 3488 $cm^{-1}$ (with a shoulder at 3460 $cm^{-1}$) and 3424 $cm^{-1}$ instead of a single band in the range 3440–3470 $cm^{-1}$ (Fig. 1.1).

Vesuvianite from the Ahkmatovskaya open pit is the only Ti-bearing VGM having space group *P*4/*n* among 33 samples investigated by Chukanov et al. (2018). The observed splitting of the band of TiO–H stretching vibrations is the result of distribution of Ti between the sites *Y*3A and *Y*3B, whereas in high-temperature VGM having the space group *P*4/*nnc* Ti is accumulated in the single *Y*3 site.

IR band in the range 3375–3380 $cm^{-1}$ which is close to the H band by Groat et al. (1995) was observed by us only for two samples with the symmetry *P*4/*n* and high contents of Cu and

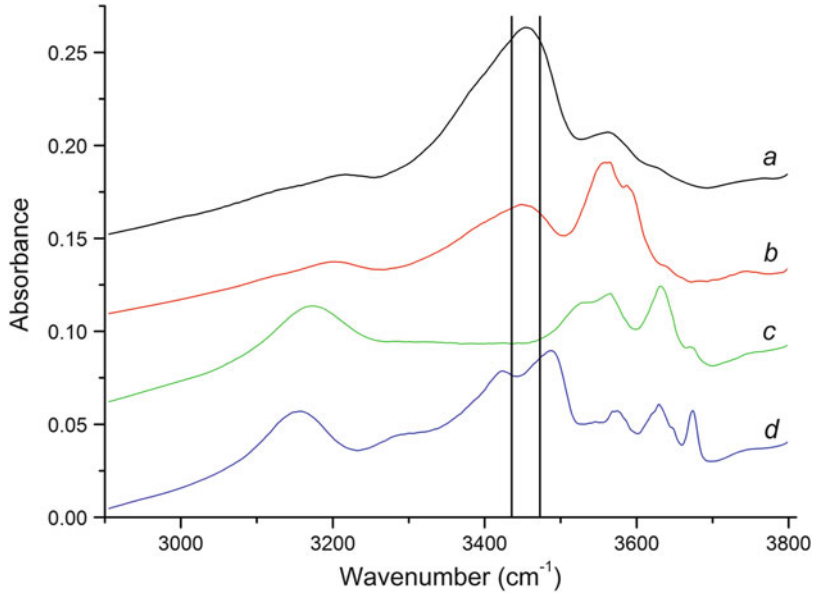


**Fig. 1.1** IR spectra of vesuvianite-group minerals with different contents of Ti in the region of O–H-stretching vibrations: a sample from Alchuri, Shigar Valley, Pakistan (Aksenov et al. 2016) with $Ti_{2.21}$ (*a*); a sample from Hazlov, Karlovy Vary Region, Czech Republic with $Ti_{0.48}$ (*b*); a sample from Myrseter area, Drammen, Buskerud, Norway with $Ti_{0.00}$ (*c*); VGM from the Ahkmatovskaya open pit, South Urals, Russia with $Ti_{1.54}$ (anomalous Ti-rich sample, space group *P*4/*n*) (*d*). Two vertical lines outline the region of the band corresponding to the Ti···O11–H1 group in *P*4/*nnc* VGM

$Mn^{3+}$. This band is more intense in the IR spectrum of the sample from the N'Chwaning III mine, Kuruman, South Africa with a relatively higher content of $Mn^{3+}$ (1.83 *apfu*). Based on these data, the band in the range 3375–3380 $cm^{-1}$ can be assigned to the $^{Y3}Mn^{3+}$···O11–H1 group.

The nominal position of the D band is 3567 $cm^{-1}$ (Groat et al. 1995), but in IR spectra of some samples this band is shifted towards lower wavenumbers (up to 3560 $cm^{-1}$). The D band is not observed in IR spectra of F-poor VGM and has the highest intensities in IR spectra of samples with most high contents of F (Britvin et al. 2003; Galuskin et al. 2003; Chukanov et al. 2018; see Fig. 1.2). Taking into account polarization $E \wedge c < 35°$ (Groat et al. 1995), the D band is to be assigned to the group O11–H1 in the situation when F occupies neighboring O11 site.

Galuskin et al. (2003) supposed that the J band corresponds to OH groups in the O10 site coordinating Fe in *Y*1 and forming hydrogen bond with F in the neighboring O10 site. However, this assumption was not confirmed by our investigations: IR spectra of most VGM, including F- and Fe-poor ones, contain distinct J band whose wavenumber varies from 3190 to 3225 $cm^{-1}$. These values correspond to strong hydrogen bonds, which is hardly possible in cases when F is the H-bond acceptor.

The weak B band (in the range from 3628 to 3632 $cm^{-1}$) is often observed in IR spectra of low-symmetry VGM. This band corresponds to very weak H-bonds formed by the groups O11–H1 with low values of the angle between O11–H1 and H1···O7 (see Lager et al. 1999).

### 1.1.2 B–O-Stretching Vibrations

In VGM boron can occupy sites with coordination numbers 3 or 4. IR spectra of most VGM samples contain shoulders in the range 1070–1170 $cm^{-1}$ corresponding to stretching vibrations of $[BO_4]$ tetrahedra.

$BO_3$ groups are connected with $Y1O6_4O10$ polyhedra *via* O10 oxygen atom to form the cluster $T2Y1O_7$ (Fig. 1.3) where $T2$ = B and $Y1 = Fe^{3+}$, $Fe^{2+}$, $Mn^{3+}$, $Cu^{2+}$, Al, or Mg. As a result, four

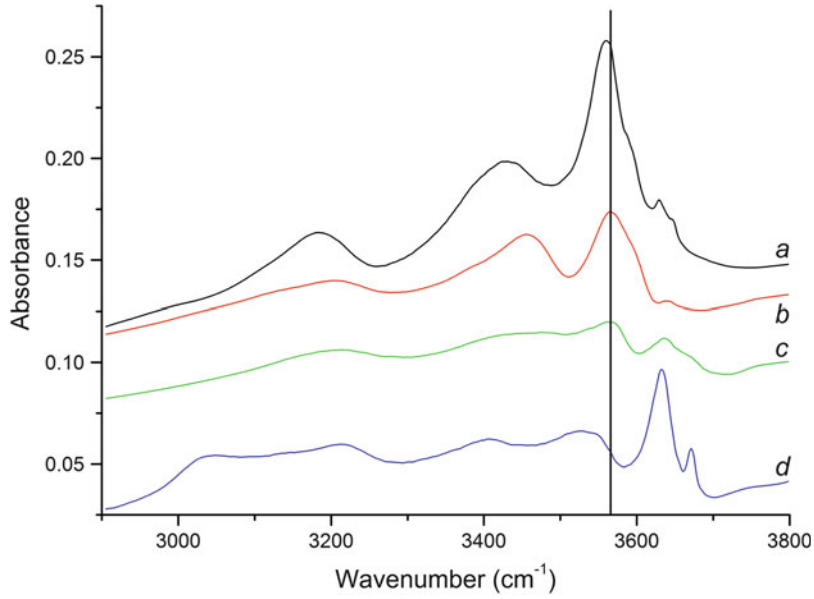


**Fig. 1.2** IR spectra of vesuvianite-group minerals with different contents of F in the region of O–H-stretching vibrations: fluorvesuvianite holotype with 7.16 *apfu* F (*a*); VGM from Sakharyok massif, Keyvy Mts., Kola Peninsula with 3.06 *apfu* F (*b*); VGM from Gulshad, Kazakhstan with 0.24 *apfu* F (*c*); F-free alumovesuvianite holotype (*d*). Vertical line corresponds to the nominal position of the D band

degrees of freedom corresponding to the bond lengths *T*2–O12 (×2), *T*2–O10, and *Y*1–O10 are involved in stretching vibrations of $BO_3^{3-}$. This results in four nondegenerate modes and, consequently, the expected number of absorption bands in the region of stretching vibrations of $BO_3$ groups (i.e., 1200–1570 $cm^{-1}$) is equal to 4. However, in the IR spectrum of wiluite only three bands are observed in this region: the peaks at 1267 and 1373 $cm^{-1}$ and the shoulder at 1415 $cm^{-1}$ (Panikorovskii et al. 2017b; see Fig. 1.4). The fourth band corresponding to symmetric vibrations of $BO_3^{3-}$ is forbidden for a regular $BO_3$ triangle and is weak in case of weak-distorted $BO_3$ triangle. The latter case takes place in wiluite: the bond lengths *T*2–O10 and *T*2–O12 are 1.39–1.40 and 1.32 Å, respectively (Panikorovskii et al. 2017b). Weak absorption between 1267 and 1373 $cm^{-1}$ may correspond to the symmetric stretching mode of $BO_3^{3-}$ groups (Fig. 1.4).

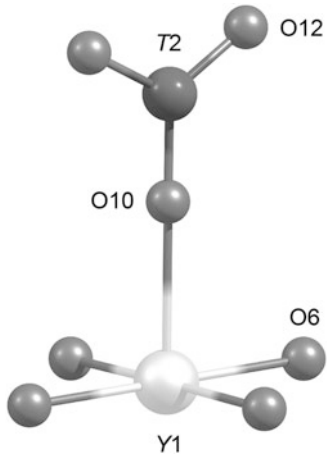


**Fig. 1.3** Local environment of the *T*2 and *Y*1 sites in vesuvianite-group minerals

Unlike wiluite, most boron-rich VGM contain significantly distorted $BO_3$ triangle. For example, in a sample from Gulshad, Kazakhstan the bond lengths *T*2–O10 and *T*2–O12 are equal to 1.384 and 1.20 Å, respectively. As a result, four distinct IR bands (at 1557, 1467, 1419, and 1365 $cm^{-1}$) are observed in the range 1200–1570 $cm^{-1}$ (curve *b* in Fig. 1.4). As compared to wiluite, these bands are substantially shifted towards high frequencies because of shorter B–O bonds and shortened *Y*1–O bond (2.044 Å for the mineral from Gulshad and 2.15 Å for wiluite: Chukanov et al. 2018; Panikorovskii et al. 2017b). These differences may be due to different predominant cations in the *Y*1 site: Mg in wiluite and $Fe^{3+}$ in the sample from Gulshad.

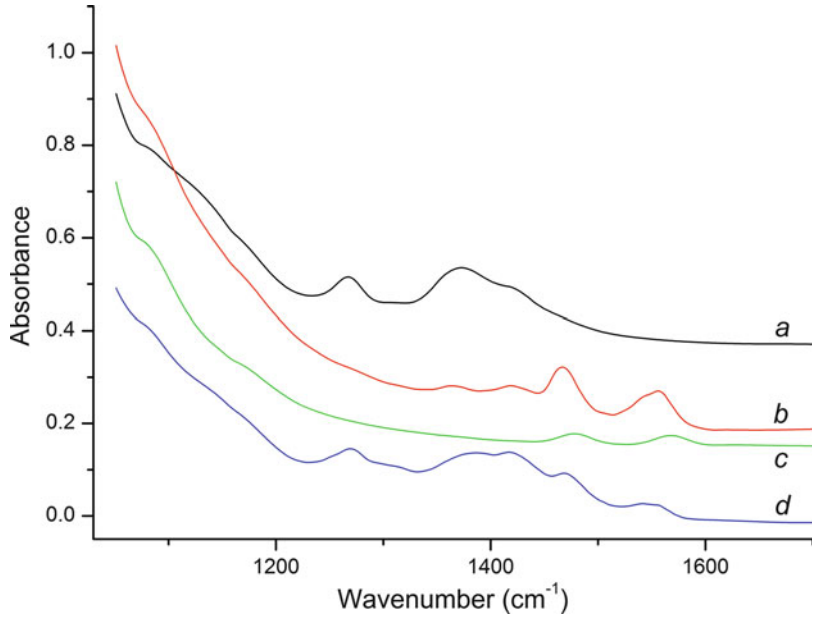


**Fig. 1.4** IR spectra of vesuvianite-group minerals in the region of B–O-stretching vibrations: wiluite from its type locality (*a*), B-rich VGM from Gulshad (*b*), a typical B-bearing vesuvianite from Somma-Vesuvius complex, Italy (*c*), and anomalous B-rich VGM from Titivskoe (*d*)

An anomalous IR spectrum with six absorption bands in the range 1200–1570 $cm^{-1}$ shows boron-rich VGM from Titivskoe boron deposit, Yakutia, Russia (curve *d* in Fig. 1.4). Structural investigation of this sample (Panikorovskii et al. 2016a) showed the presence of domains with different symmetry (*P*4/*nnc* and *P*4/*n*).

### 1.1.3 Stretching and Bending Vibrations of $SiO_4^{4-}$ and $Si_2O_7^{6-}$ Groups

Based on the available data on IR spectra of a restricted set of VGM Kurazhkovskaya and Borovikova (2003) concluded that for low-symmetry samples the band of Si–O-stretching vibrations in the range from 960 to 990 $cm^{-1}$ is shifted on 10–15 $cm^{-1}$ towards lower frequencies as compared to high-symmetry VGM. Our data confirm this conclusion only partly. Indeed, among nine samples with the space group *P*4/*n*, eight samples show strong IR bands in the range 962–968 $cm^{-1}$, and in the IR spectrum of one more sample a band at 973 $cm^{-1}$ is observed. Among 21 boron-poor samples with the space group *P*4/*nnc*, for 16 samples bands in the range 976–986 $cm^{-1}$ are observed, but 5 samples show bands between 962 and 968 $cm^{-1}$.

Another specific feature of low-symmetry VGM indicated by Kurazhkovskaya and Borovikova (2003), as well as by Borovikova and Kurazhkovskaya (2006) is the doublet ~575 +615 $cm^{-1}$ corresponding to O–Si–O bending vibrations. This regularity was confirmed by us as a general trend; however, among 21 boron-poor samples with the space group *P*4/*nnc*, 3 samples show doublets in the range ~575–615 $cm^{-1}$ with components of approximately equal intensity.

## 1.2 Problem of Melanophlogite

Melanophlogite is a clathrate compound which contains guest molecules $N_2$, $CO_2$, and $CH_4$ entrapped within the cages of the 3D framework built by $SiO_4$ tetrahedra (Gies 1983; Nakagawa et al. 2001; Kolesov and Geiger 2003). The cubic unit cell of the structure of melanophlogite includes two $[5^{12}]$ cages and six $[5^{12}6^2]$ cages (Fig. 1.5). The former are considered to be occupied mainly by $CH_4$ molecules and the latter by $N_2$ and $CO_2$ (Gies et al. 1982; Gies 1983). In

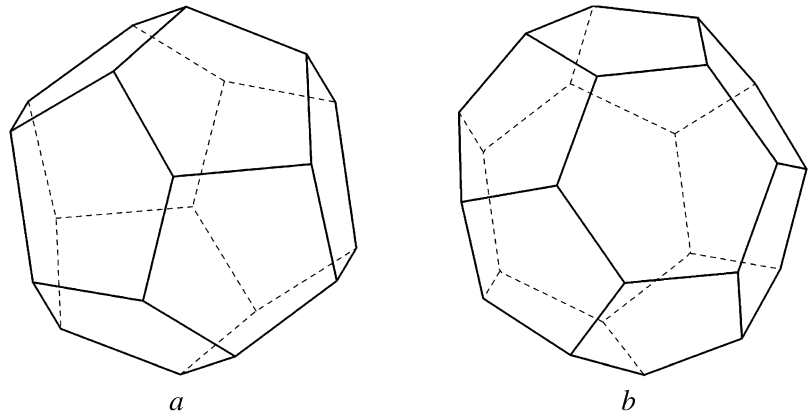


**Fig. 1.5** [$5^{12}$] cages (**a**) and [$5^{12}6^2$] cages (**b**) in the structure of melanophlogite

melanophlogite from Mt. Hamilton, California, USA, the occupancy factor of the $CH_4$ site in the [$5^{12}$] cage is about 90% (Gies 1983). The molecules of carbon dioxide located in the [$5^{12}6^2$] cages can rotate and are statistically distributed between 12 possible equivalent orientations. Most part of $N_2$ and $CO_2$ occurs in the [$5^{12}6^2$] cage, but minor part of these molecules can be present in the [$5^{12}$] cage (Gies 1983; Kolesov and Geiger 2003). Based on the available structural data, the general formula of melanophlogite can be written as follows: $(CH_4, N_2,CO_2)_{2-x}(N_2,CO_2)_{6-y}(Si_{46}O_{92})$.

The IR spectrum of melanophlogite from Fortullino, Livorno province, Tuscany, Italy (cubic, with $a = 13.4051(13)$ Å, according to single-crystal X-ray diffraction data) contains a strong band at 2330–2336 $cm^{-1}$ corresponding to antisymmetric vibrations of $CO_2$ molecules (Chukanov and Chervonnyi 2016; see Fig. 1.6).

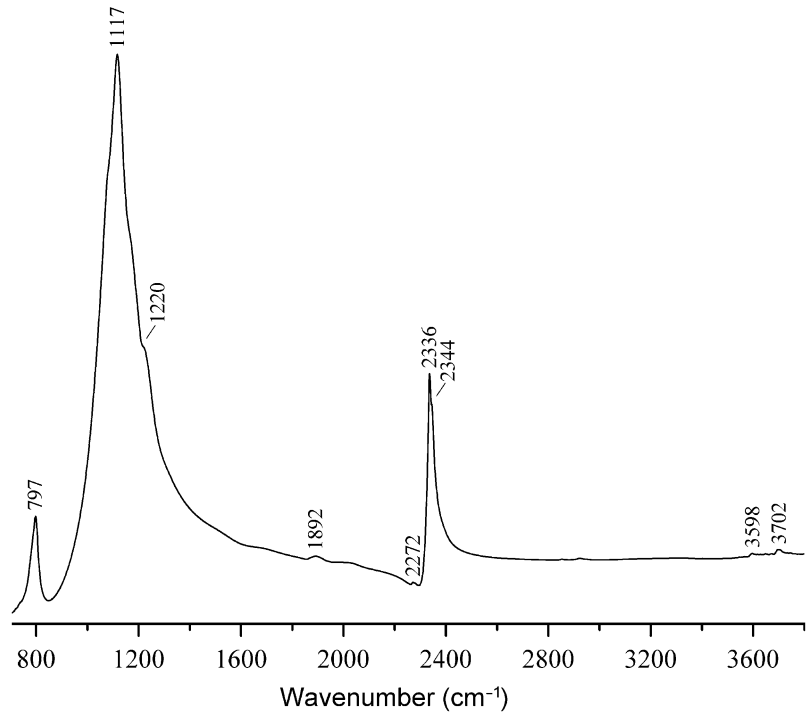


**Fig. 1.6** Powder IR spectrum of melanophlogite from Fortullino, Italy

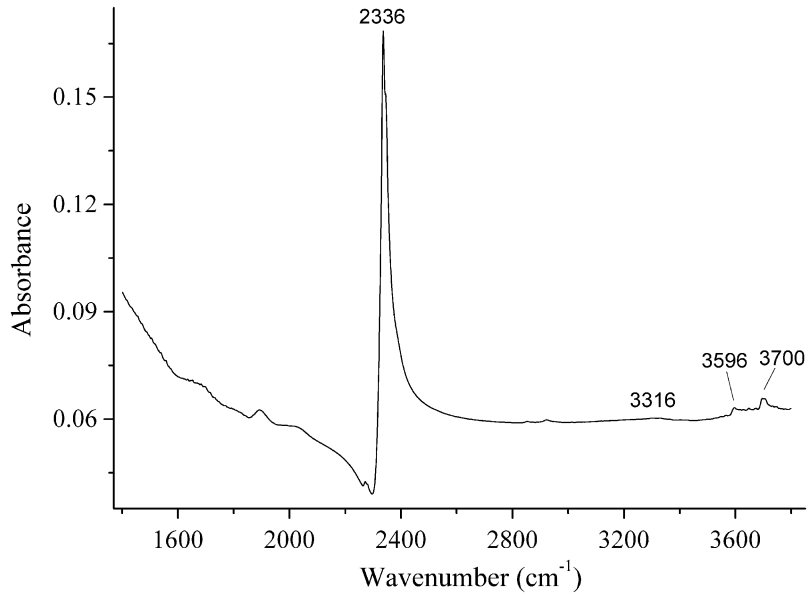


**Fig. 1.7** IR spectrum of melanophlogite from Fortullino in the 1400–3800 $cm^{-1}$ range. Very weak bands in the range from 2800 to 3000 $cm^{-1}$ correspond to grease impurity

A weaker peak at ~2375 $cm^{-1}$ present it IR spectra of some melanophlogite samples from this locality (Chukanov 2014) may be due to rotational splitting or correspond to a minor amount of $CO_2$ molecules in the $[5^{12}]$ cages, which are predominantly occupied by $CH_4$. Weak bands at 3700 and 3596 $cm^{-1}$ (Fig. 1.7) are, respectively, due to asymmetric and symmetric stretching vibrations of $H_2O$ molecules that do not form hydrogen bonds. The band at 3316 $cm^{-1}$ can be tentatively assigned to silanol groups or H-bonded $H_2O$ molecules.

Two $CO_2$ modes at 1277 and 1378 $cm^{-1}$ observed in the Raman spectrum of melanophlogite from Mt. Hamilton, California, USA correspond to the first overtone of the $\nu_2$-bending mode and the symmetric $\nu_1$-stretching mode, respectively, both bands being components of a vibrational system coupled via Fermi resonance (Kolesov and Geiger 2003).

Raman spectrum of melanophlogite from Mt. Hamilton has been investigated previously at 4 K (Kolesov and Geiger 2003). The bands at 2900 and 2909 $cm^{-1}$ in the single-crystal Raman spectrum of melanophlogite from this locality have been assigned to asymmetric stretching modes of $CH_4$ located in the $[5^{12}]$ and $[5^{12}6^2]$ cages, respectively. Along with the main band at 1378.5 $cm^{-1}$ assigned to $CO_2$ molecules in the $[5^{12}6^2]$ cages, the shoulder at 1376 $cm^{-1}$ was registered and was attributed to $CO_2$ in the $[5^{12}]$ cages. Kolesov and Geiger (2003) also reported the presence of the band of symmetric N≡N-stretching vibrations located at 2321 $cm^{-1}$ which corresponds to $N_2$ molecules. The IR forbidden band of $N_2$ in binary mixtures with other molecules has been observed at about 2328 $cm^{-1}$ (Bernstein and Sandford 1999). It is to be noted that this value is close to the wavenumber of antisymmetric vibrations of $CO_2$ molecules, which is forbidden in Raman spectra. However, this band is not observed by us in Raman spectra of melanophlogite from different Italian localities (Figs. 1.8, 1.9 and 1.10).

Raman spectrum of the sample from Fortullino (Fig. 1.8) exhibits strong bands of $CO_2$ at 1277 and 1383 $cm^{-1}$. Two weak bands at 1257 and 1398 $cm^{-1}$ accompanying the components of the Fermi-doublet are the so-called hot bands arising from the transitions from an excited vibrational level to the ground vibrational level (Wang et al. 2011). In accordance with Frezzotti et al. (2012) and Wang et al. (2011), carbon dioxide in this mineral is in the high density fluid state with $D \approx 1$ g/$cm^3$. This is confirmed by the down shift of the Fermi doublet frequencies from 1388

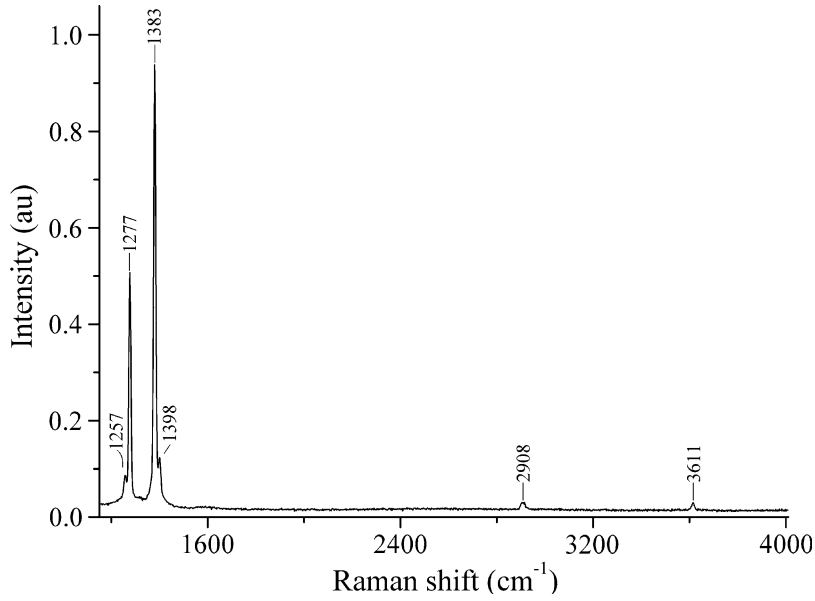


**Fig. 1.8** Raman spectrum of melanophlogite from Fortullino

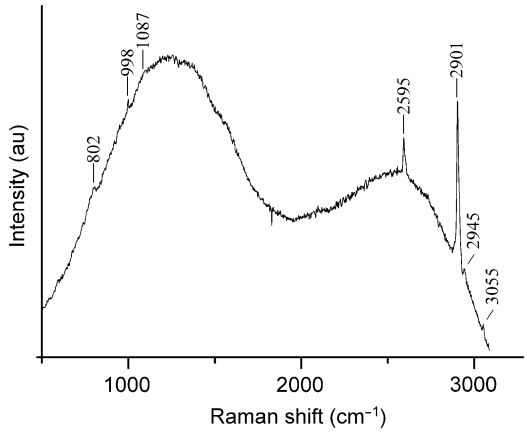


**Fig. 1.9** Raman spectrum of melanophlogite from Racalmuto

and 1285 $cm^{-1}$ ($\Delta = 103$ $cm^{-1}$) for $CO_2$ at normal conditions to the values 1383 and 1277 $cm^{-1}$ ($\Delta = 106$ $cm^{-1}$); the increased value of $\Delta$ in the spectrum of melanoflogite from Fortullino (Fig. 1.8) also corresponds to a high-density $CO_2$ fluid. The very weak band at 2908 $cm^{-1}$ which is attributed to $CH_4$ and the band at 3611 $cm^{-1}$ attributed to OH-groups are in a good agreement with the IR spectrum of this sample (Chukanov and Chervonnyi 2016). Thus, nitrogen, which is a substantial component in melanophlogite from Mt. Hamilton, is absent in the sample from Rio Fortullino.

Melanophlogite from Racalmuto, Sicily (Fig. 1.9) is characterized by a higher content of $CH_4$ detected by the bands at 2901 and 3055 $cm^{-1}$ and by a trace amount of $C_2H_6$ detected by the very weak bands at 998 and 2945 $cm^{-1}$ (Kohlrausch 1943; Momma et al. 2011). The presence of $H_2S$ molecules is detected by the presence in the Raman spectrum of the band at 2595 $cm^{-1}$. This sample does not contain $N_2$ and $CO_2$ molecules in detectable amounts. The sample of melanophlogite from Racalmuto contains a small amount of mineral impurities of calcite or aragonite (the band at 1087 $cm^{-1}$: Edwards et al. 2005) and celestine (998 $cm^{-1}$: Frezzotti et al. 2012). The weak band at 802 $cm^{-1}$ and the bands at 363 and 276 $cm^{-1}$ relate to the spectrum of the melanophlogite-type silicon-oxygen framework.

Melanophlogite from Miniera Giona, Sicily (Fig. 1.10) contains $H_2S$ molecules (the band of H–S-stretching vibrations at 2593 $cm^{-1}$) and a low amount of $CH_4$ molecules (2904 $cm^{-1}$) whereas bands of $N_2$ and $CO_2$ are not observed in its Raman spectrum. This sample contains anhydrite admixture detected by the Raman bands at 1132 and 1004 $cm^{-1}$ (Frezzotti et al.

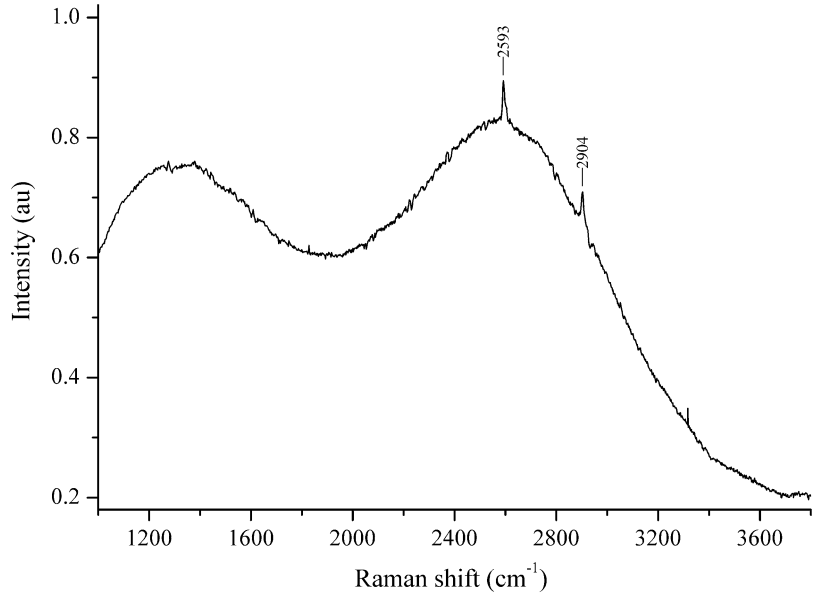


**Fig. 1.10** Raman spectrum of melanophlogite from Miniera Giona

2012). Broad peaks in Figs. 1.9 and 1.10 are due to fluorescence.

Powder IR spectra of melanophlogite from some other localities do not show any presence of methane molecules. In the frequency range from 2800 to 3000 $cm^{-1}$, a sample from Chvaletice, Bohemia shows the presence of three overlapping, relatively broad bands indicative of the contamination by a polyatomic aliphatic hydrocarbon, most probably grease. Similar but much weaker bands are present in the IR spectrum of melanophlogite from Fortullino, Italy (Fig. 1.7), but no characteristic bands of methane are observed in this spectrum too.

The IR spectra of melanophlogite samples from Racalmuto and Miniera Giona (Fig. 1.11) show much lower contents of $CO_2$ (the bands at 2337–2338 $cm^{-1}$) and substantially higher contents of $CH_4$ (the bands at 3005–3008 $cm^{-1}$) as compared with the sample from Fortullino. Moreover, the bands in the range from 2850 to 2950 $cm^{-1}$ in the IR spectrum of melanophlogite samples from Miniera Giona indicate the presence of hydrocarbons heavier than methane. IR spectrum of the sample from Racalmuto confirms the presence of $H_2S$ (Fig. 1.12).

The band assignment and the distribution of different components between $[5^{12}]$ and $[5^{12}6^2]$ cages in melanophlogite samples from different localities are given in Table 1.1. These examples show that, in all probability, melanophlogite is not a single mineral species, but a mineral group including minerals with different combinations of small molecules ($CO_2$, $CH_4$, $H_2S$, $N_2$, $H_2O$, $C_2H_6$) entrapped in the $[5^{12}]$ and $[5^{12}6^2]$ cages. In particular, the mineral from Fortullino may be the $CO_2$-dominant analogue of melanophlogite, and in the samples from Racalmuto and Miniera Giona $H_2S$ may be a species-defining component.

## 1.3 Problem of Nakauriite

Nakauriite was initially described as a new mineral with the general formula $(Mn,Ni,Cu)_8(SO_4)_4(CO_3)(OH)_6{\cdot}48H_2O$ (Suzuki et al. 1976). The mineral occurs in fissure-fillings in brucite-bearing serpentine at Nakauri, Aichi Prefecture, Japan, and is intimately intergrown with chrysotile. Most analytical data for nakauriite, including powder X-ray diffraction pattern, chemical composition and IR spectrum, have been obtained for a polymineral mixture, in

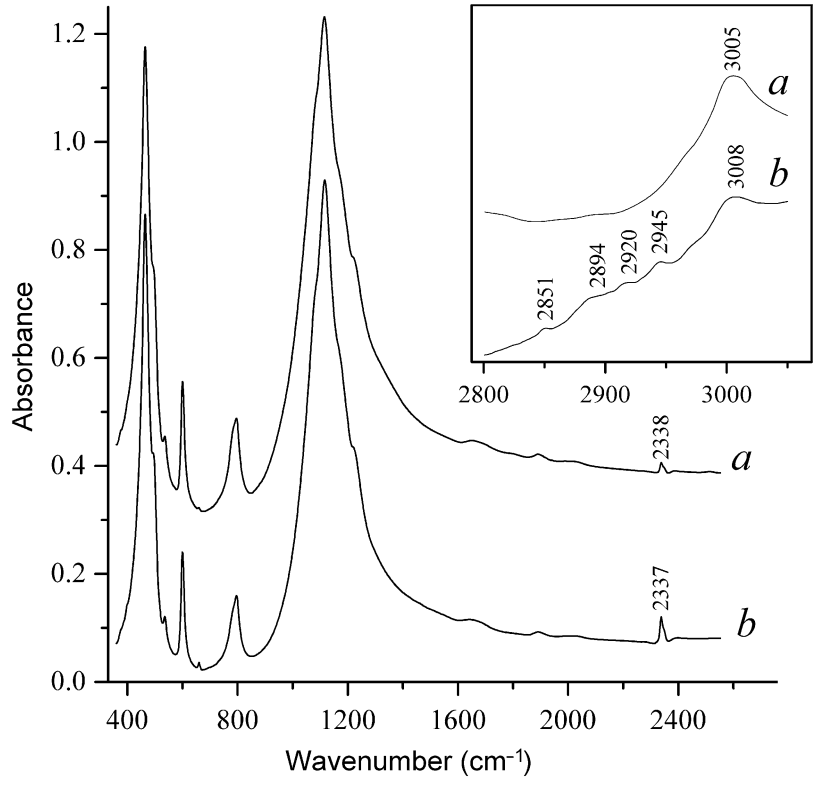


**Fig. 1.11** Powder IR spectra of melanophlogite from Racalmuto (*a*) and Miniera Giona (*b*)

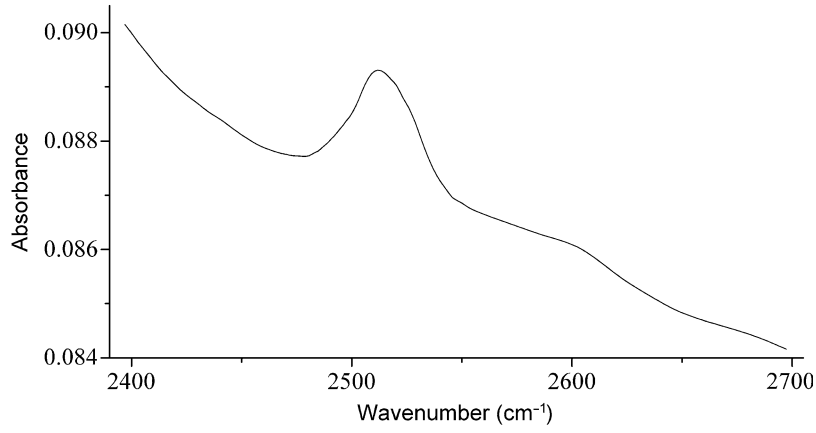


**Fig. 1.12** IR spectrum of melanophlogite from Racalmuto in the region of S–H-stretching vibrations

which chrysotile is the main phase. The above formula does not conform to analytical data of Suzuki et al. (1976). Taking into account strong predominance of Cu over Mn and Ni, the simplified formula $Cu_8(SO_4)_4(CO_3)(OH)_6{\cdot}48H_2O$ is given for nakauriite in the IMA list of minerals. Published IR spectrum of nakauriite from its type locality contains strong bands of admixed chrysotile at 1075, 950 and 613 $cm^{-1}$ (Suzuki et al. 1976; see curve *a* in Fig. 1.13), but characteristic bands of sulfate anions are not observed.

Later nakauriite was reported from several localities in Great Britain, USA, Austria, Italy, and Russia (Braithwaite and Pritchard 1983;

**Table 1.1** The assignment of IR and Raman bands and the distribution of different enclathrated components between $[5^{12}]$ and $[5^{12}6^2]$ cages for melanophlogite samples from different localities

| Locality | Wavenumber ($cm^{-1}$) | Assignment |
|---|---|---|
| Mt. Hamilton[a] | 3050w (R) | $CH_4$ (first overtone of the doubly degenerate $\nu_2$-bending mode?) |
| | 2909w (R) | $CH_4$ in $[5^{12}6^2]$ (symmetric stretching mode) |
| | 2900 (R) | $CH_4$ in $[5^{12}]$ (symmetric stretching mode) |
| | 2321 (R) | $N_2$ in $[5^{12}6^2]$ |
| | 1378.5 (R) | $CO_2$ in $[5^{12}6^2]$ (symmetric stretching mode) |
| | 1376 (R) | $CO_2$ in $[5^{12}]$ (symmetric stretching mode) |
| | 1277 (R) | $CO_2$: Fermi resonance between symmetric stretching mode and first overtone of the bending mode |
| Fortullino | 3700 (IR) | $H_2O$ (antisymmetric stretching mode) |
| | 3611 (R) | $H_2O$ (?) O–H-stretching mode |
| | 3596 (IR) | $H_2O$ (symmetric stretching mode) |
| | 3316 (IR) | $H_2O$ (?) O–H-stretching mode (H-bonded OH) |
| | 2908w (R) | $CH_4$ in $[5^{12}6^2]$ |
| | 2344 (IR) | $^{12}CO_2$ in $[5^{12}]$ (antisymmetric stretching mode) |
| | 2336 (IR) | $^{12}CO_2$ in $[5^{12}6^2]$ (antisymmetric stretching mode) |
| | 2273w (IR) | $^{13}CO_2$ (antisymmetric stretching mode) |
| | 1398w (R) | $CO_2$ ("hot band") |
| | 1383 (R) | $CO_2$ in $[5^{12}6^2]$ (symmetric stretching mode) |
| | 1377 (R) | $CO_2$ in $[5^{12}]$ (symmetric stretching mode) |
| | 1277 (R) | $CO_2$: Fermi resonance between symmetric stretching mode and first overtone of the bending mode |
| | 1257w (R) | $CO_2$ ("hot band") |
| Racalmuto | 3055w (R) | Hydrocarbon other than methane |
| | 3005w (IR) | $CH_4$ in $[5^{12}]$ (asymmetric stretching mode) |
| | 2945w (R) | $C_2H_6$? |
| | 2901 (R) | $CH_4$ in $[5^{12}]$ (symmetric stretching mode) |
| | 2595 (R) | $H_2S$ (symmetric stretching mode) |
| | 2512 (IR) | $H_2S$ (antisymmetric stretching mode) |
| | 2338w (IR) | $^{12}CO_2$ in $[5^{12}6^2]$ (antisymmetric stretching mode) |
| Miniera Giona | 3008w (IR) | $CH_4$ in $[5^{12}]$ (asymmetric stretching mode) |
| | 2945w (IR) | Hydrocarbon other than methane |
| | 2920w (IR) | Hydrocarbon other than methane |
| | 2904w (R) | $CH_4$ in $[5^{12}]$ (symmetric stretching mode) |
| | 2894w (IR) | Hydrocarbon other than methane |
| | 2851w (IR) | Hydrocarbon other than methane |
| | 2593 (R) | $H_2S$ (symmetric stretching mode) |
| | 2337 (IR) | $^{12}CO_2$ in $[5^{12}6^2]$ (antisymmetric stretching mode) |

*R* Raman spectrum, *IR* infrared spectrum, *w* weak band
[a]Data from Kolesov and Geiger (2003)

Barnes 1986; Postl and Moser 1988; Palenzona and Martinelli 2007; Popov et al. 2016), as well as a secondary product in metallurgic slags. All available data indicate that nakauriite (1) does not contain sulfate anion and (2) usually forms fine intergrowths with magnesium serpentine-group minerals (see curve *b* in Fig. 1.13). In particular, electron microprobe analyses of nakauriite from Japan and from Nevada (Peacor et al. 1982) do not show substantial amounts of sulfur. Microchemical tests show only traces of $SO_4^{2-}$ (Braithwaite and Pritchard 1983).

We managed to obtain an almost pure fraction of nakauriite from its type locality. Its IR

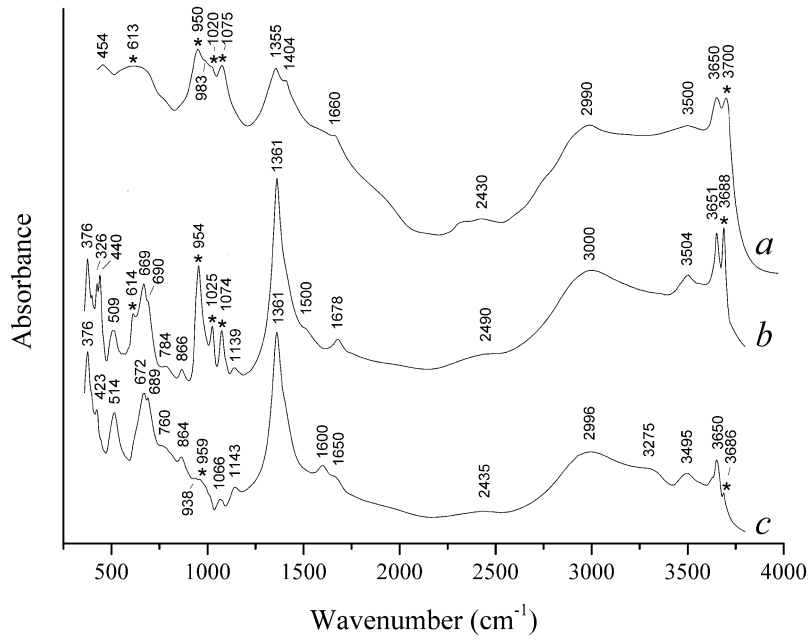


**Fig. 1.13** IR spectra of nakauriite-bearing samples from Nakauri drawn using data from Suzuki et al. (1976) (*a*), and from Karkodin, South Urals, Russia (*b*) and IR spectrum of an almost pure nakauriite from Nakauri (*c*). Bands of admixed serpentine are marked by asterisk

spectrum is given in Fig. 1.13 (curve *c*). Specific features of the mineral are unusually low frequency of the non-split band of C–O-stretching vibrations (1361 $cm^{-1}$), as well as relatively low intensity and high width of the band of out-of-plane bending vibrations of $CO_3^{2-}$ groups at 864 $cm^{-1}$. The bands at 1600 and 1650 $cm^{-1}$ indicate the presence of $H_2O$ molecules. The same features are inherent in carbonate members of the hydrotalcite group (Chukanov 2014) whose structures contain brucite-like layers and interlayer $CO_3^{2-}$ anions and water molecules. Weak bands at 1066 and 1143 $cm^{-1}$ may be due to the presence of trace amounts of $SO_4^{2-}$ anions.

Our electron microprobe analyses of nakauriite samples from Nakauri (Japan), Karkodin, (Russia) and Monte Ramazzo mine (Italy) show that this mineral is Mg-dominant. Only three metal cations have been found, namely Mg, $Cu^{2+}$, and $Ni^{2+}$. The atomic ratio Mg:Cu:Ni in a sample from Nakauri is 0.75:0.23:0.02. In another sample from Nakauri Mg:Cu:Ni = 0.80:0.19:0.01. In the sample from Karkodin Mg:Cu:Ni = 0.75:0.23:0.02. Nakauriite from Monte Ramazzo does not contain Ni in detectable amounts; Mg:Cu = 0.80:0.20. In all analyzed samples the content of sulfur is below its detection limit. The predominance of Mg over Cu in nakauriite from Karkodin was noted also by Popov et al. (2016).

Thermal data for nakauriite from Suzuki et al. (1976) are nearly consistent with the general simplified formula $(Mg_3Cu^{2+})(OH)_6(CO_3)\cdot 4H_2O$. Hypothetically, nakauriite can be an interstratification of brucite and copper carbonate modules. Powder X-ray diffraction data of nakauriite from South Urals kindly provided by I.V. Pekov are given in Table 1.2.

Suzuki et al. (1976) reported the absence of the reflection near 7.8 Å in some samples from Nakauri. It was supposed that this reflection may be due to an impurity (Peacor et al. 1982; Braithwaite and Pritchard 1983). However, nakauriite from Karkodin shows a relatively strong reflection at 7.88 Å (Table 1.2). In our opinion, the reflections at 7.32 and 7.88 Å may correspond to nakauriite-type phases with different contents of interlayer water.

A further detailed investigation of nakauriite and revision of its chemical formula are required.

**Table 1.2** Powder X-ray diffraction data of nakauriite from Karkodin, South Urals, Russia (MoKα radiation)

| *d*, Å | *I*, % | *d*, Å | *I*, % | *d*, Å | *I*, % |
|---|---|---|---|---|---|
| 7.88 | 19 | 2.845 | 4 | 1.5947 | 1 |
| 7.32 | 100 | 2.677 | 4 | 1.5762 | 1 |
| 5.11 | 12 | 2.612 | 8 | 1.5447 | 12 |
| 4.835 | 17 | 2.536 | 4 | 1.5185 | 5 |
| 4.629 | 12 | 2.365 | 43 | 1.5107 | 4 |
| 4.485 | 14 | 2.258 | 7 | 1.4569 | 5 |
| 4.217 | 4 | 2.221 | 4 | 1.4210 | 3 |
| 3.928 | 12 | 2.096 | 1 | 1.4035 | 3 |
| 3.642 | 13 | 2.037 | 2 | 1.3523 | 1 |
| 3.539 | 15 | 1.956 | 3 | 1.2985 | 4 |
| 3.335 | 6 | 1.910 | 24 | 1.2910 | 4 |
| 3.305 | 8 | 1.820 | 2 | 1.2404 | 1 |
| 3.105 | 4 | 1.782 | 3 | 1.2281 | 2 |
| 3.065 | 4 | 1.7206 | 4 | 1.2170 | 2 |
| 2.976 | 3 | 1.6951 | 2 | 1.2021 | 2 |
| 2.939 | 3 | 1.6657 | 2 | 1.1973 | 2 |
| 2.874 | 4 | 1.6439 | 5 | 1.1082 | 1 |

## 1.4 Relationship Between Nepskoeite and Shabynite

Nepskoeite was initially described as a new chloride-hydroxide mineral with the formula $Mg_4Cl(OH)_7{\cdot}6H_2O$ (Apollonov 1998). However, IR spectrum of nepskoeite published by Apollonov (1998) contains very strong band at 1297 $cm^{-1}$ corresponding to stretching vibrations of orthoborate groups, as well as distinct band at $cm^{-1}$ that may correspond to bending vibrations of orthoborate groups (Fig. 1.14).

Our reinvestigation of nepskoeite from the type material confirmed the presence of boron in this mineral. In particular, IR spectrum contains strong bands at 1301 and 734 $cm^{-1}$ corresponding to stretching and bending vibrations of $BO_3^{3-}$ anions, respectively (Chukanov 2014; see Fig. 1.15). Moreover, color reaction with quinalizarin shows a high content of boron in nepskoeite.

IR spectrum of nepskoeite shows similarity with that of shabynite $Mg_5(BO_3)(Cl,OH)_2(OH)_5{\cdot}4H_2O$ (Fig. 1.16). In particular, the IR spectrum of shabynite contains strong bands at 1302 and 732 $cm^{-1}$. However, substantial differences between these spectra are observed in the region of vibrations of $H_2O$ molecules above 1500 $cm^{-1}$.

There is also close similarity between powder X-ray diffraction (PXRD) patterns of nepskoeite and shabynite (Table 1.3). However, nepskoeite shows strong reflections at 10.64 and 3.498 $cm^{-1}$ that are absent in the PXRD pattern of shebynite. On the other hand, strongest reflections of different shabynite samples are observed at 9.62 and 3.191 $cm^{-1}$. Refraction indices of nepskoeite ($\alpha = 1.532$, $\beta \approx \gamma = 1.562$) are somewhat lower than those of shabynite ($\alpha = 1.543$, $\beta = 1.571$, $\gamma = 1.577$).

Based on these data, nepskoeite can be tentatively considered as a hydrous orthoborate chloride, a high-hydrated analogue of shabynite. Both minerals need further investigations, first of all, determination of unit-cell dimensions and $H_2O$ content by means of direct methods.

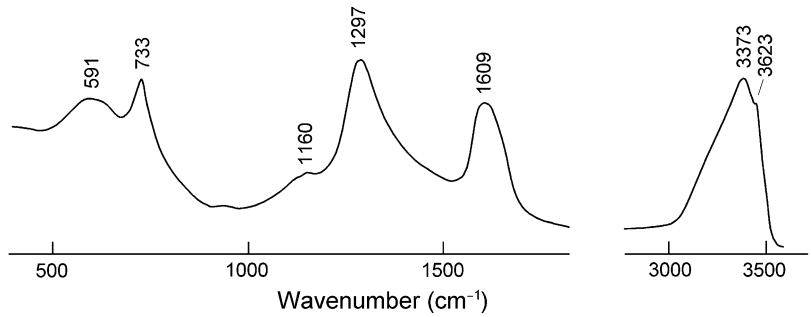


**Fig. 1.14** IR spectrum of nepskoeite drawn using data from Apollonov (1998)

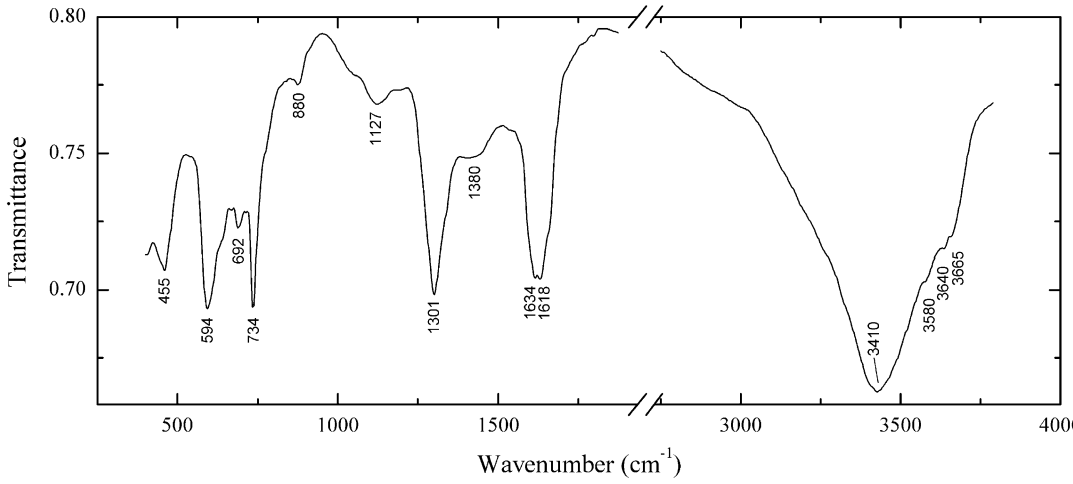


**Fig. 1.15** IR spectrum of nepskoeite drawn using data from Chukanov (2014)

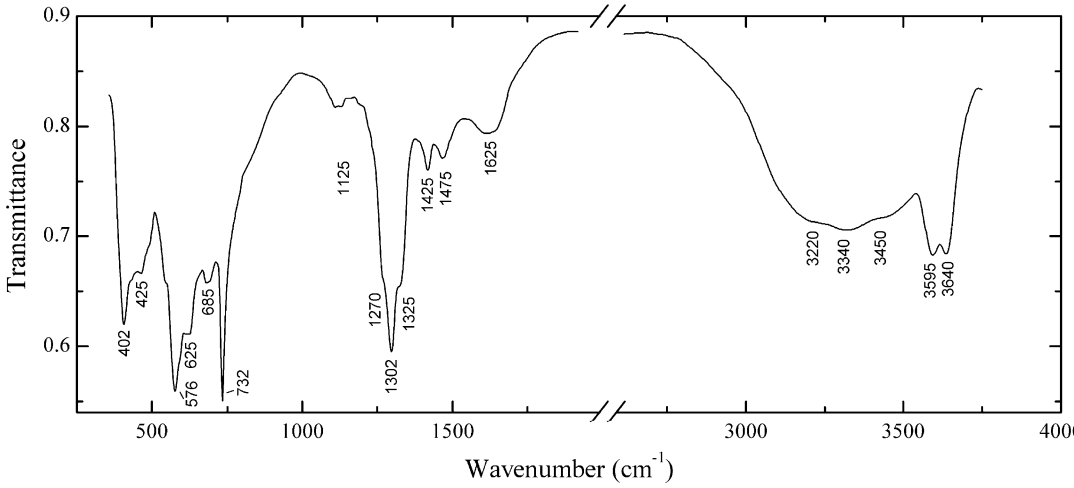


**Fig. 1.16** IR spectrum of shabynite drawn using data from Chukanov (2014)

## 1.5 Orthoborate Groups in Lead Carbonate Minerals

The $CO_3^{2-}$ and $BO_3^{3-}$ anions have the same trigonal planar configuration, but in most orthoborate and carbonate minerals these groups do not show appreciable isomorphous substitutions. The main causes of the absence of isomorphous substitutions between these groups are differences in their charges and sizes. In addition, $BO_3^{3-}$ groups are often significantly distorted (see, e.g., Kolitsch et al. 2012, as well as Sect. 1.1). However, some lead carbonate minerals are exceptions from this regularity. For example, IR spectra of some samples of molybdophyllite $Pb_8Mg_9(Si_{10}O_{28})(CO_3)_3(OH)_8O_2.H_2O$, which is nominally a boron-free mineral, show weak IR bands of B–O-stretching vibrations at 1170 and 1240 $cm^{-1}$) (Fig. 1.17), whereas Raman spectrum of the structurally investigated molybdophyllite sample does not show bands of borate groups (Kolitsch et al. 2012).

The crystal structure of molybdophyllite (Kolitsch et al. 2012) does not contain boron-

**Table 1.3** Strongest lines (with $I \geq 10\%$) of the PXRD patterns of nepskoeite and shabynite

| Nepskoeite (Apollonov 1998) | | Shabynite, sample No. 3 (Pertsev et al. 1980) | |
|---|---|---|---|
| *d*, Å | *I*, % | *d*, Å | *I*, % |
| 11.41 | 29 | 11.33 | 10 |
| 10.64 | 18 | –[a] | –[a] |
| 9.78 | 46 | 9.72 | 17 |
| 9.60 | 38 | – | – |
| 5.57 | 17 | – | – |
| 5.48 | 16 | 5.48<br>5.41 | 16<br>16 |
| – | – | 4.86 | 19 |
| 4.78 | 15 | 4.77 | 19 |
| 4.25 | 20 | 4.266<br>4.230 | 16<br>17 |
| – | – | 4.133 | 29 |
| 3.726 | 15 | 3.726 | 17 |
| 3.624 | 14 | 3.648 | 10 |
| 3.498 | 100 | – | – |
| – | – | 3.191 | 100 |
| 3.184 | 10 | – | – |
| 2.977 | 10 | – | – |
| 2.739 | 16 | – | – |
| 2.448 | 18 | 2.447 | 19 |
| 2.395 | 17 | 2.390 | 11 |
| 2.284 | 11 | – | – |
| 1.749 | 10 | – | – |

[a]The strongest reflection of the powder X-ray diffraction pattern of shabynite sample No. 2 (Pertsev et al. 1980) is observed at 9.62 Å

dominant sites and, consequently, $BO_3^{3-}$ anions occur in $CO_3^{2-}$-dominant positions, unlike roymillerite $Pb_{24}Mg_9(Si_9AlO_{28})(SiO_4)(BO_3)(CO_3)_{10}(OH)_{14}O_4$ and britvinite $Pb_{15}Mg_9(Si_{10}O_{28})(CO_3)_2(BO_3)_4(OH)_{12}O_2$, in which orthoborate and carbonate groups are ordered in different sites (Yakubovich et al. 2008; Chukanov et al. 2017b; see Fig. 1.18).

The IR spectrum of hydrocerussite $Pb_3(OH)_2(CO_3)_2$ from Långban (curve *b* in Fig. 1.19) contains weak bands at 1230 (shoulder), 742, and 470 $cm^{-1}$. These bands may be assigned to stretching and bending vibrations of orthoborate anions partly substituting regular $CO_3$ triangles in the hydrocerussite structure. Indeed, in the IR spectrum of fluoborite containing regular $BO_3$ triangle strong bands of B–O-stretching and O–B–O bending vibrations are observed at 1241, 743, and 468 $cm^{-1}$ (Chukanov 2014). It is important to note that bands of orthoborate groups are absent in the IR spectra of hydrocerussite from Merehead quarry, England (curve *a* in Fig. 1.19), some related minerals (curves *c* and *d* in Fig. 1.19), as well as synthetic analogues of hydrocerussite and plumbonacrite (Brooker et al. 1983). In all probability, the presence of borate groups in hydrocerussite from Långban is the result of high activity of boron that accompanied formation of this deposit where different borate minerals are common.

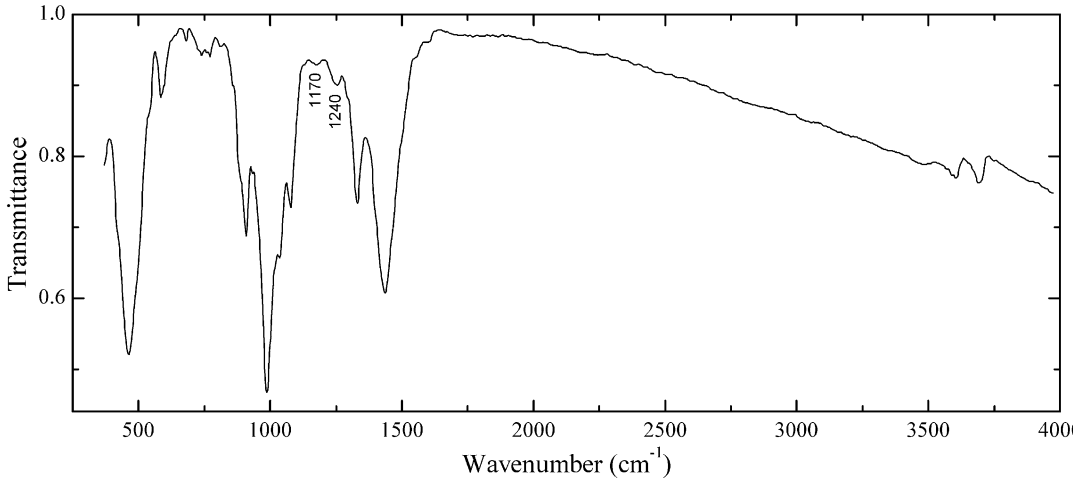


**Fig. 1.17** IR spectrum of molybdophyllite from the Långban deposit, Bergslagen ore region, Filipstad district, Värmland, Sweden (Chukanov 2014, sample Sil247). The wavenumbers of $BO_3^{3-}$ groups are indicated

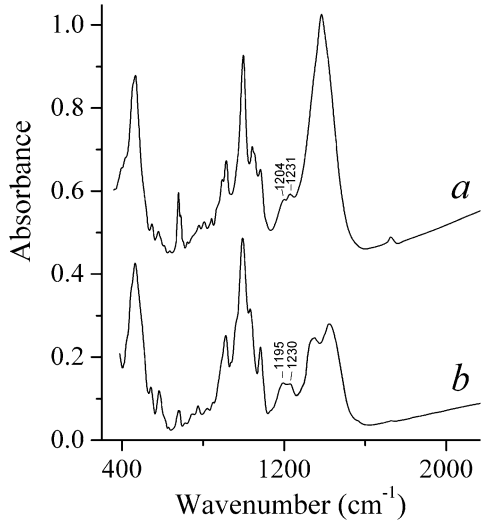


**Fig. 1.18** IR spectra of (*a*) roymillerite and (*b*) britvinite from Långban, Värmland, Sweden. Bands of stretching vibrations of $BO_3^{3-}$ groups are indicated

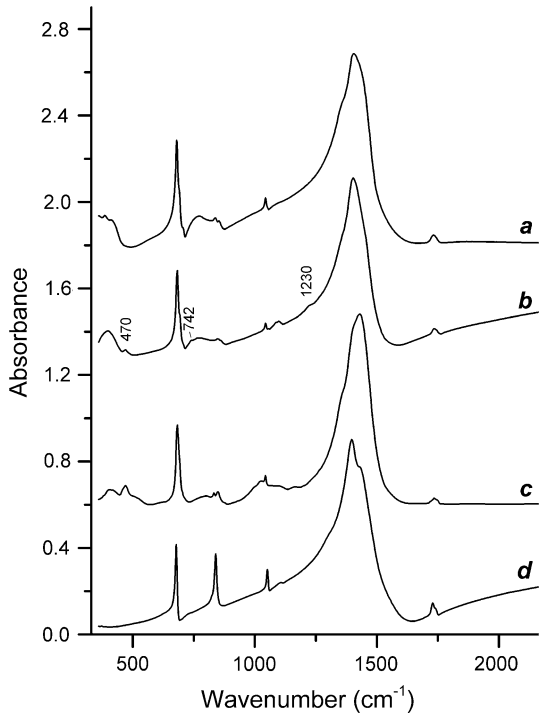


**Fig. 1.19** IR spectra of (*a*) hydrocerussite from Merehead quarry, (*b*) hydrocerussite from Långban, (*c*) hydrocerussite-related phase $NaPb_5(CO_3)_4(OH)_3$ from Lavrion, and (*d*) cerussite from Merehead quarry. Bands of $BO_3^{3-}$ groups are indicated

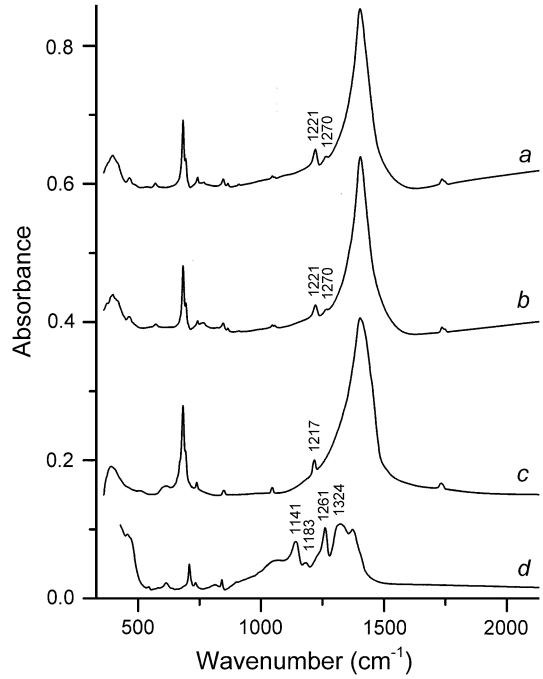


**Fig. 1.20** IR spectra of (*a*) plumbonacrite from Merehead quarry, (*b*) plumbonacrite from Långban, (*c*) somersetite, and (*d*) mereheadite. Bands of stretching vibrations of $BO_3^{3-}$ groups are indicated

The IR spectra of plumbonacrite $Pb_5O(OH)_2(CO_3)_3$ from Merehaad and Långban (Fig. 1.20) are similar and differ from the IR spectra of synthetic plumbonacrite analogue (Brooker et al. 1983) by additional bands of $BO_3^{3-}$ groups at 1270, 1221, 742, and 464–465 $cm^{-1}$. Unlike hydrocerussite, a mineral with the only site of $CO_3^{2-}$ groups, in the crystal structure, plumbonacrite is characterized by five positions of carbonate groups (Krivovichev and Burns 2000). The IR spectrum of plumbonacrite contains two bands of asymmetric B–O-stretching vibrations (at 1270 and 1221 $cm^{-1}$), which indicates the presence of $BO_3^{3-}$ groups in different sites.

The IR spectrum of somersetite (curve *c* in Fig. 1.20) is similar to those of plumbonacrite and hydrocerussite and contains bands of $BO_3^{3-}$ groups at 1217 and 738 $cm^{-1}$. The crystal structure of somersetite consists of electroneutral $[Pb_3(OH)_2(CO_3)_2]$ hydrocerussite block and electroneutral $[Pb_5O_2(CO_3)_3]$ block with the structure derivative from plumbonacrite. The

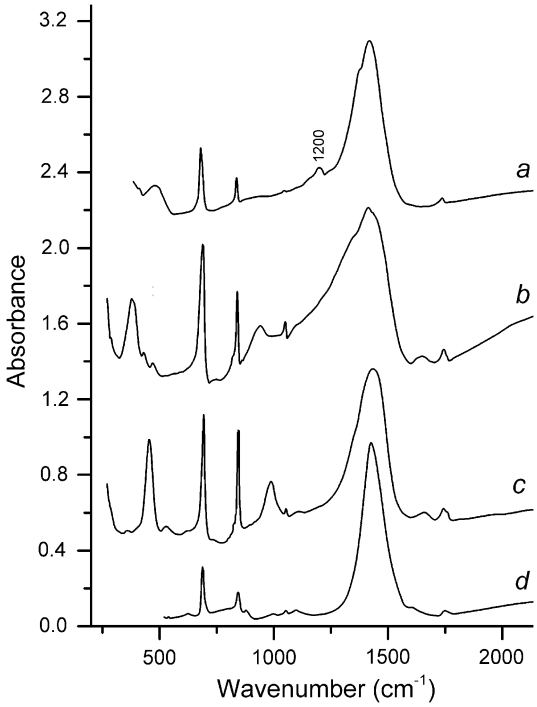


**Fig. 1.21** IR spectra of (*a*) grootfonteinite holotype, (*b*) synthetic compound $KPb_2(CO_3)_2(OH)$ (Brooker et al. 1983), (*c*) synthetic compound $NaPb_2(CO_3)_2(OH)$ (Brooker et al. 1983), and (*d*) abellaite holotype (Ibáñez-Insa et al. 2017). Band of stretching vibrations of $BO_3^{3-}$ groups is indicated

only band of B–O-stretching vibrations observed in the IR spectrum of somersetite indicates that all admixed $BO_3^{3-}$ groups belong to the hydrocerussite block.

The relatively weak bands at 480 and 1200 $cm^{-1}$ in the IR spectrum of grootfonteinite $Pb_3O(CO_3)_2$ indicate the presence of minor amounts of undistorted orthoborate groups, but these groups are absent in most samples of structurally related minerals and compounds (see Fig. 1.21).

In hydrocerussite, plumbonacrite, somersetite, and grootfonteinite $CO_3/BO_3$ are undistorted. As a result, bands of admixed B–O-stretching vibrations of $BO_3^{3-}$ anions are observed in the narrow wavenumber range from 1200 to 1270 $cm^{-1}$. In contrast to these minerals, in mereheadite $Pb_{47}O_{24}(OH)_{13}Cl_{25}(BO_3)_2(CO_3)$ $BO_3$ triangles are significantly distorted with B–O distances varying from 1.23 to 1.32 Å (Krivovichev et al. 2009). This results in splitting of the band of B–O-stretching vibrations into several components (at 1141, 1183, and 1261 $cm^{-1}$); in addition, broad band at 1324 $cm^{-1}$ corresponding to a mixed mode involving B–O- and C–O-stretching vibrations appears (curve *d* in Fig. 1.20).